OPTIMIZATION OF INTERNAL FORCES IN FORCE–CLOSURE GRASPS

ANTONIO BICCHI† DOMENICO PRATTICHIZZO‡ GIANNI ANTOGNETTI†

†*Centro "E. Piaggio", Università di Pisa, via Diotisalvi* 2, 56100 *Pisa, Italia*

‡*Dipartimento di Ingegneria dell'Informazione, Università di Siena, via Roma* 56, 53100 *Siena, Italia*

bicchi@piaggio.ccii.unipi.it, prattichizzo@ing.unisi.it

The control of internal forces is paramount in robotics grasping. In force closure grasps internal forces can be controlled in order to prevent the object from possible slippage due to external disturbances. A cost function approach to compute the internal force is proposed. The cost function weights the distance of the contact force from the friction constraints and from the maximum and minimum force levels allowable in the system. A globally asymptotically convergent algorithm returns the optimal internal grasp forces which will be used as the reference of a force control loop.

1 Introduction

The robotic hand can be viewed as the paradigm of the more general scenario of multiple mechanisms simultaneously interacting with the same object or reference link. In this framework, the term "grasp" usually refers to the ability of holding the object in a stable way in spite of external wrenches exerted on the object. The main subject in grasping analysis is the determination of contact forces able to counter–balance the external wrench and to maximize the distance of the contact forces from the contact constraints which for force–closure grasps are the friction and the unilateral constraints [1].

One of the early works in such a subject was by Orin and Oh [3]. They linearized the friction constraint and used standard linear programming (LP) techniques to find the contact forces as a function of the disturbance and constraints parameters. Later Nakamura *et al.* [4], introduced the nonlinear programming techniques to select the grasping forces. More recently a cost function approach for internal force optimization was proposed in [1] and [5]. The cost function was built as a weighted summation of terms taking into account the distance from violating contact constraints and its convexity was proved. Buss *et al.* [6] solved the problem of grasping force optimization in a context where friction and force balance constraints are described by equivalent to the positive definite matrices.

In this paper, the cost function approach to the optimal synthesis of internal forces is used. A globally asymptotically convergent algorithm returning the optimal internal grasp force is proposed. Experimental activity on a testbed comprised of a two–fingered developed at the Centro "E. Piaggio" is finally described.

2 Dynamic model

Consider a robotic hand grasping an object by means of m kinematic chains interacting with the object at n contacts. Let $\mathbf{q} \in \mathbb{R}^q$ denote the vector of joint positions, and let $\mathbf{u} \in \mathbb{R}^d$ be the vector describing the position and orientation of a frame attached to the object. Correspondingly, let $\tau \in \mathbb{R}^q$ be the vector of forces and torques of the joint actuators, and $\mathbf{w} \in \mathbb{R}^d$ the vector of forces and torques resultant from actions applied directly at the object.

Hand and object dynamics are linked through n rigid–body unilateral contact constraints which, according to [7], can be written in terms of the grasp matrix $\mathbf{G}$ and the hand Jacobian $\mathbf{J}$ as

$$\begin{bmatrix} \mathbf{J} & -\mathbf{G}^{\mathrm{T}} \end{bmatrix} \begin{bmatrix} \dot{\mathbf{q}} \\ \dot{\mathbf{u}} \end{bmatrix} = 0. \tag{1}$$

The number t of constraint equations depends on the models used to describe the n contact interactions [8,9].

By introducing a t–dimensional vector $\mathbf{t}$ of Lagrangian multipliers and by differentiating (1), rigid–body dynamics equations are obtained as

$$\begin{cases} \mathbf{M}_h(\mathbf{q})\ddot{\mathbf{q}} + \mathbf{Q}_h(\mathbf{q}, \dot{\mathbf{q}}) + \mathbf{J}^{\mathrm{T}}\mathbf{t} = \tau; \\ \mathbf{M}_o(\mathbf{u})\ddot{\mathbf{u}} + \mathbf{Q}_o(\mathbf{u}, \dot{\mathbf{u}}) - \mathbf{G}\mathbf{t} = \mathbf{w}; \\ \mathbf{J}\ddot{\mathbf{q}} - \mathbf{G}^{\mathrm{T}}\ddot{\mathbf{u}} + \mathbf{Q}_c(\mathbf{q}, \dot{\mathbf{q}}, \mathbf{u}, \dot{\mathbf{u}}) = 0, \end{cases} \tag{2}$$

where $\mathbf{Q}_c = \frac{\partial \mathbf{J}\dot{\mathbf{q}}}{\partial \mathbf{q}}\dot{\mathbf{q}} - \frac{\partial \mathbf{G}^{\mathrm{T}}\dot{\mathbf{u}}}{\partial \mathbf{u}}\dot{\mathbf{u}}$, $\mathbf{M}_h(\cdot)$ and $\mathbf{M}_o(\cdot)$ are symmetric and positive definite inertia matrices and $\mathbf{Q}_h(\cdot,\cdot)$ and $\mathbf{Q}_o(\cdot,\cdot)$ are terms including velocity-dependent and gravity forces of the hand and of the object, respectively. Observe that the Lagrangian multiplayer $\mathbf{t}$ represent the vector of forces exerted at the contact constraints.

Rigid–body dynamics equation (2) can be written as

$$\mathbf{M}_{\mathrm{dyn}} \begin{bmatrix} \ddot{\mathbf{q}} \\ \ddot{\mathbf{u}} \\ \mathbf{t} \end{bmatrix} = \begin{bmatrix} \tau - \mathbf{Q}_h \\ \mathbf{w} - \mathbf{Q}_o \\ \mathbf{Q}_c \end{bmatrix}, \tag{3}$$

where

$$\mathbf{M}_{\mathrm{dyn}} = \begin{bmatrix} \mathbf{M}_h & 0 & \mathbf{J}^{\mathrm{T}} \\ 0 & \mathbf{M}_o & -\mathbf{G} \\ \mathbf{J} & -\mathbf{G}^{\mathrm{T}} & 0 \end{bmatrix}. \tag{4}$$

In order for this equation to completely determine the law of motion of the system, it is necessary that matrix M_{dyn} be invertible. Such case is analyzed in detail in [10]. For all manipulation systems with non–invertible M_{dyn}, i.e., for hyperstatic grasps having $\ker(J^T) \cap \ker(G) \neq 0$ the rigid–body dynamics (3) fails to determine the law of motion of the complete system. For a whole analysis of hyperstatic grasps the reader is referred to [7].

3 Internal force control

The prior task in robotic grasping is the control of grasping forces, usually referred to as "internal forces". Internal forces play a fundamental role in controlling the manipulation task. Whenever the resultant of a disturbance action on the object contacts is in the tangential direction, the manipulator cannot reject such a disturb by simply opposing a contact force. It must generate an additional internal force to keep the total contact force in the friction cone and to not violate contact constraints.

From the object dynamics and (2), one can write

$$\widetilde{w} = G^T t \tag{5}$$

where $\widetilde{w} = -w + M_o(u)\ddot{u} + Q_o(u, \dot{u})$ is the sum of external (disturbance) forces and of dynamical forces. Assuming perfect tracking of the given object trajectory in spite of external wrenches, the corresponding contact forces solve equation (5). However, in general, such solution is underdetermined, since the grasp matrix G has a non trivial null–space referred to as subspace of internal forces. The term "internal" forces is used as these forces are self–balanced and do not affect the object dynamics.

The general solution of (5) is

$$t = G^R \widetilde{w} + Ay, \tag{6}$$

where G^R is a right-inverse (G is supposed to be full row rank) providing a particular solution, A is a matrix whose columns form a basis of the nullspace of the grasp matrix and y is the vector describing a homogeneous solution in the base A.

The freedom in choosing the internal part of the contact force (6) allows to optimize the grasp with regard to several concerns provided that the internal force is controllable. In fact, in general, not all the contact forces can be controlled by the joint inputs. The problem has been put into evidence in [11] and a detailed analysis for grasps with contact compliance is reported in [9].

Consider a non–hyperstatic grasp, $(\ker(J^T) \cap \ker(G) = 0)$. After a block matrix inversion, it ensues that the relationship between the contact force vector and input vectors

$$\begin{aligned} t = {} & T\left(JM_h^{-1}\tau - G^T M_o^{-1} w\right) \\ & -T\left(JM_h^{-1}Q_h - G^T M_o^{-1} Q_o - Q_c\right) \end{aligned} \tag{7}$$

where $T = \left(JM_h^{-1}J^T + G^T M_o^{-1} G\right)^{-1}$.

Equation (7) describes the contact forces reachable by joints inputs τ and external wrenches w in a rigid–body non–hyperstatic grasp. Among these forces the internal ones are obtained projecting t onto the nullspace of the grasp matrix. Their characterization is straightforward.

Proposition 1 *Consider an initial non–hyperstatic equilibrium. The whole subspace of internal forces,* $\ker(G)$, *is reachable by joint torques*

$$\ker(G) = \mathcal{T}_\tau \cap \ker(G).$$

The subspace $\mathcal{T}_\tau$ *is the subspace of reachable* t*'s by joint torques*

$$\mathcal{T}_\tau = \left(JM_h^{-1}J^T + G^T M_o^{-1} G\right)^{-1} \mathrm{im}\left(JM_h^{-1}\right).$$

Proof . Simply observe that

$$\begin{aligned} & \left(JM_h^{-1}J^T + G^T M_o^{-1} G\right) \ker(G) \cap \mathrm{im}\left(JM_h^{-1}\right) \\ & \quad = \left(JM_h^{-1}J^T + G^T M_o^{-1} G\right) \ker(G), \end{aligned} \tag{8}$$

and multiplying (8) by T, the proposition is proved. □

4 Contact forces constraints

Constraints (1) do not take into account neither the unilateral nature of contact constraints nor the contact slippage, i.e., the violation of the cones limits for friction constraints. In other words equation (1) holds provided that the contact force t fulfill the unilateral and friction constraints.

In this paper the degrees of freedom Ay in choosing the contact forces (6) are exploited to reduce the risk of violating the unilateral, the friction constraints and a constraint on the maximum contact force.

Observe that a delicate object could be damaged by too large grasp forces. In some cases, it is some parts of the robot system (e.g. the force sensors) that might be hurt. A safety threshold, depending on the object being manipulated, should be chosen to limit the intensity of contact forces. Another reason for limiting contact forces is actuator saturation. At the contact i, the **maximum contact force** constraint is

$$\|p_i\| \leq f_{i,max} > 0, i = 1, 2, \ldots, n. \tag{9}$$

where p_i is the contact force at the i-th contact $(t^T = [p_1 \cdots p_n])$, and $\|\cdot\|$ indicates the euclidean norm of the argument.

There are also reasons to keep contact forces above a minimum positive value. One is the unilateral nature of mechanical contacts. Another is that contact sensors

work better in a certain range of forces, and cannot distinguish too small forces from noise. Note that a lower bound on contact forces allows to avoid the temporal discontinuity of contacts. The lower bound on the normal component of contact forces can be imposed through the **Minimum contact force** constraint

$$\mathbf{p}_i^T \mathbf{n}_i \geq f_{i,min} > 0, \quad i = 1, 2, \ldots, n. \tag{10}$$

where $\mathbf{n}_i$ is the unit normal vector to the surfaces at the i-th contact point.

In the absence of local torques, the normal and tangential components of each contact force $\mathbf{p}_i$ must comply with **friction limits** of Coulomb's law

$$\mathbf{p}_i^T \mathbf{n}_i \geq \frac{1}{\mu_i} \| (\mathbf{I} - \mathbf{n}_i \mathbf{n}_i^T) \mathbf{p}_i \| = \alpha_i \|\mathbf{p}_i\|, \tag{11}$$

where μ_i is the static friction coefficient in the current contact conditions, and $\alpha_i = (1 + \mu_i^2)^{-1/2}$.

When a complete soft finger model of contact is assumed, friction limits involve more complex relationships [6]. In this paper, it is assumed for simplicity that only hard-finger contacts are present in the grasp.

5 Cost Function

An efficient algorithm to evaluate the optimizing grasp forces, based on a cost function with some desirable properties, is defined.

Constraints (9), (10), and (11) on the i-th contact force can be written in the single form

$$\sigma_{i,j}(\mathbf{y}, \widetilde{\mathbf{w}}) = \alpha_{i,j} \|\mathbf{p}_i\| + \beta_{i,j} \mathbf{p}_i^T \mathbf{n}_i + \gamma_{i,j} \leq 0, \tag{12}$$

where $\alpha_{i,1} = 1$, $\beta_{i,1} = 0$, and $\gamma_{i,1} = -f_{i,max}$ for maximum force constraints; $\alpha_{i,2} = 0$, $\beta_{i,2} = -1$, and $\gamma_{i,2} = f_{i,min}$ for minimum force constraints; and $\alpha_{i,3} = \alpha_i$, $\beta_{i,3} = -1$, and $\gamma_{i,3} = 0$ for friction constraints. Let $\Omega_{i,j}^{\kappa} \subset \Re^h$ indicate the set of grasp variables $\mathbf{y}$ that, in the presence of a given load $\widetilde{\mathbf{w}}$, satisfies constraints in (12) of corresponding indices with a small margin $\kappa \geq 0$,

$$\Omega_{i,j}^{\kappa} = \{\mathbf{y} \mid \sigma_{i,j}(\mathbf{y}) < -\kappa\}.$$

Note that the region where all the contact constraints are satisfied,

$$\Omega^0 = \bigcap_{i,j} \Omega_{i,j}^0, \tag{13}$$

contains

$$\Omega^k = \bigcap_{i,j} \Omega_{i,j}^k$$

i.e., the set where the contact constraints are fulfilled with a guaranteed margin k.

Consider the cost function given by the weighted summation

$$V_k(y, w) = \Sigma_{i=1}^{n} \Sigma_{j=1}^{3} \omega_{i,j} V_{k\,i,j}$$

$$V_{i,j}(\mathbf{y}, \mathbf{w}) = \begin{cases} (2\,\sigma_{i,j}^2)^{-1} & \mathbf{y} \in \Omega_{i,j}^{\kappa} \\ a\,\sigma_{i,j}^2 + b\,\sigma_{i,j} + c & \mathbf{y} \notin \Omega_{i,j}^{\kappa} \end{cases} \tag{14}$$

with $a = \frac{3}{2\kappa^2}$, $b = \frac{4}{\kappa^3}$, and $c = \frac{3}{\kappa^2}$.

It has been shown [1] that the penalty function (14) is twice continuously differentiable and strictly convex with respect to $\mathbf{y} \in \mathbb{R}^h$. Note that for $k = 0$ components $V_{i,j}$ in (14) turn into

$$V_{i,j}(\mathbf{y}, \mathbf{w}) = \begin{cases} (2\,\sigma_{i,j}^2)^{-1} & \mathbf{y} \in \Omega_{i,j}^0; \\ \infty & \mathbf{y} \notin \Omega_{i,j}^0. \end{cases}$$

Standard optimization techniques can be employed to search the unique minimum

$$\widehat{\mathbf{y}}_k = \arg\min_{\mathbf{y}} V_k(\mathbf{y}, \widetilde{\mathbf{w}}).$$

The following update law:

$$\dot{\mathbf{y}}(t) = -\zeta \frac{\partial^2 V}{\partial y^2}^{-1} \frac{\partial V}{\partial y}; \tag{15}$$

where

$$\zeta = \lambda + \frac{\frac{\partial V}{\partial w}^T \dot{\widetilde{\mathbf{w}}}(t)}{\frac{\partial V}{\partial y}^T \frac{\partial^2 V}{\partial y^2}^{-1} \frac{\partial V}{\partial y}}, \lambda > 0.$$

provides a globally asymptotically convergent algorithm. A proof of convergence is straightforwardly obtained by considering the time derivative of the positive-definite Lyapunov candidate function V

$$\begin{aligned} \dot{V} &= \frac{\partial V}{\partial y}^T \dot{\mathbf{y}} + \frac{\partial V}{\partial w}^T \dot{\mathbf{w}} \\ &= -\zeta \frac{\partial V}{\partial y}^T \frac{\partial^2 V}{\partial y^2}^{-1} \frac{\partial V}{\partial y} + \frac{\partial V}{\partial w}^T \dot{\mathbf{w}} \\ &= -\lambda \frac{\partial V}{\partial y}^T \frac{\partial^2 V}{\partial y^2}^{-1} \frac{\partial V}{\partial y} \leq 0. \end{aligned} \tag{16}$$

Recalling that $\frac{\partial^2 V}{\partial y^2}$ is positive definite for any $\mathbf{y} \in \Re^h$, the only possible equilibrium point is for $\frac{\partial V}{\partial y} = 0$, i.e., at the optimum.

Although the optimization algorithm (16) has been discussed in the continuous time domain, it is easy to derive its discrete time version.

6 Optimization

To obtain an optimum grasp in spite of external forces $\widetilde{\mathbf{w}}$, the grasp controller must be able to evaluate, in case the set Ω^0 (13) would not be void, the optimum

$$\widehat{\mathbf{y}}_0 = \arg\min_{\mathbf{y}} V_0(\mathbf{y}, \widetilde{\mathbf{w}}). \tag{17}$$

Note that for $k = 0$ the penalty function (14) is strictly convex only in Ω^0 and the recursive optimization algorithm (15) works provided that the initial $\mathbf{y}$ belongs to Ω^0 whose characterization by elements is a difficult task because of nonlinear relationships.

The next proposition will help to use penalty functions V_k to compute the optimum (17).

Proposition 2 *Compute $\widehat{\mathbf{y}}_{\bar{k}}$, the minimum of $V_{\bar{k}}$. Sufficient condition for $\widehat{\mathbf{y}}_0 = \widehat{\mathbf{y}}_{\bar{k}}$. is that*

$$\widehat{\mathbf{y}}_{\bar{k}} \in \Omega^{\bar{k}}.$$

Proof . For every $k < \bar{k}$, Ω^k is a subset of $\Omega^{\bar{k}}$. Then, being the minimum of V_k global, it ensues that, for each $k < \bar{k}$, $\widehat{\mathbf{y}}_k = \widehat{\mathbf{y}}_{\bar{k}}$ and

$$\widehat{\mathbf{y}}_0 = \lim_{k \to 0} \arg\min_{\mathbf{y}} V_k(\mathbf{y}, \widetilde{\mathbf{w}}) = \widehat{\mathbf{y}}_{\bar{k}}.$$

□

Unfortunately, in some cases the sufficient condition of Proposition 2 is not fulfilled. This may happen

[C1] if the chosen margin $\bar{k}$ is so large that $\widehat{\mathbf{y}}_{\bar{k}}$ does not fall into $\Omega^{\bar{k}}$, even if Ω^0 is not void, or

[C2] if the set Ω^0 itself is void which means that there is not any feasible internal force able to counter–balance, by force closure, the external wrench.

The problem of the optimum grasp synthesis consists in detecting these two different situations and, more in general, it can be stated as

Problem 1 *For any external wrench $\widetilde{\mathbf{w}}$, determine if $\Omega^0 = \emptyset$ or $\Omega^0 \neq \emptyset$ and in this last case find the optimal solution $\widehat{\mathbf{y}}_0$.*

Problem 1 is attacked by reducing the margin k and re–running the optimization algorithm until it ends finding the optimum $\widehat{\mathbf{y}}_0$ or concluding that $\Omega^0 = \emptyset$.

6.1 Taylor expansion and minimization procedure

Assume that

$$\Omega^0 \neq \emptyset, \tag{18}$$

i.e., the global optimum $\widehat{\mathbf{y}}_0$ exists. Moreover assume that, for a given k, the optimization algorithm (15) returns $\widehat{\mathbf{y}}_k$. It is easy to verify that each component of the vector

$$\Delta\widehat{y} = \widehat{y}_k - \widehat{y}_0 \tag{19}$$

only depends on k and that its Taylor expansion, with residual, of order 0 around $k = 0$ is, $(0 < \xi_i < 1)$

$$\Delta\widehat{y}_i(k) = \Delta\widehat{y}_i(0) + k\frac{\partial\Delta\widehat{y}_i}{\partial k}\bigg|_{\xi_i} = k\frac{\partial\Delta\widehat{y}_i}{\partial k}\bigg|_{\xi_i}.$$

Once $\widehat{\mathbf{y}}_k$ is evaluated, the residual of the Taylor expansion provides lower and upper bounds on each component of the optimum vector $\widehat{\mathbf{y}}_0$,

$$\widehat{y}_{k_i} - \Delta k_i \leq \widehat{y}_{0_i} \leq \widehat{y}_{k_i} + \Delta k_i \tag{20}$$

where

$$\Delta k_i = \left| \sup_{0<\xi_i<k} k\frac{\partial\Delta\widehat{y}_i}{\partial k}\bigg|_{\xi_i} \right|. \tag{21}$$

and, from the theorem of implicit function,

$$\begin{aligned}\frac{\partial\Delta\widehat{y}_i}{\partial k}\bigg|_{\substack{k=\xi_i \\ y=\widehat{y}_k}} &= \left[\frac{\partial}{\partial k}\left(\operatorname{argmin}_{\mathrm{y}} \mathrm{V_k}\right)\right]_i\bigg|_{\substack{k=\xi_i \\ y=\widehat{y}_k}} \\ &= \left[-\left(\frac{\partial^2 V_k}{\partial y^2}\right)^{-1}\frac{\partial^2 V_k}{\partial y\,\partial k}\right]_i\bigg|_{\substack{k=\xi_i \\ y=\widehat{y}_k}}\end{aligned}$$

The next proposition deals with the detection of condition C2. It is simply proved observing that (20) is a direct consequence of assumption (18).

Proposition 3 *Assume that, for a given k_j, the cost function $\mathrm{V_{k_j}}$ is minimized by y_{k_j}. Necessary and sufficient conditions for $\Omega^0 = \emptyset$ is that any element of the hyper–rectangle*

$$\mathcal{Y}_{k_j} = \{\mathbf{y} : \widehat{\mathbf{y}}_{k_j} - \Delta_{k_j} \leq \mathbf{y} \leq \widehat{\mathbf{y}}_{k_j} + \Delta_{k_j}\}$$

violate the contact constraints (12) at all contacts, i.e.,

$$\forall \mathbf{y} \in \mathcal{Y}_{k_j}, \forall i, j \qquad \sigma_{i,j}(\mathbf{y}, \widetilde{\mathbf{w}}) > 0. \tag{22}$$

Note that checking condition (22) can be reduced to a problem of convex optimization [2].

Starting from propositions 2 and 3, a simple procedure to solve Problem 1 is stated:

Procedure:

step 0 choose a margin $\bar{k}$ and set $k_i = \bar{k}$;
step 1 computes $\widehat{\mathbf{y}}_{k_i}$;
step 2 if Proposition 2 holds then $\widehat{\mathbf{y}}_0 = \widehat{\mathbf{y}}_{k_i}$ and stop;
step 3 else if condition (22) is satisfied, $\Omega^0 = \emptyset$ and stop;
step 4 otherwise set $k_i = k_i/m$, $m > 0$ and go back to step 1.

The procedure ends satisfying Proposition 2 or concluding that $\Omega^0 = \emptyset$.

7 Experiment

The experiments testbed developed at Centro "E. Piaggio" is a new hand designed for both force/position control and nonholonomic motion planning experiments. The hand, pictorially described in fig. 1 consists of two fingers whose fingertips are disks rotating around two axes: $a1$ and $a2$. Two four-bar-linkage inserted in the

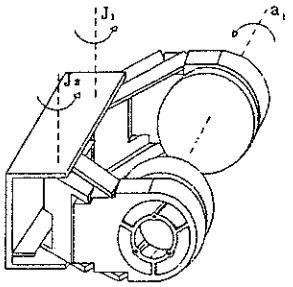

Figure 1: The 4–dof hand developed at Centro "E. Piaggio", University of Pisa.

kinematic chains of the fingers are able to keep the fingertip axes parallel one each other. The mechanism of the two fingers can rotate around two parallel joints: $j1$ and $j2$. The whole device has 4 degrees of freedom, namely $(\theta_{j1}, \theta_{j2})$ and $(\theta_{a1}, \theta_{a2})$ actuated by two DC motors and two step–by–step motors and sensorized by two servo–potentiometers and two encoders, respectively. Observe that in the experiments, fingertip angle are kept constant by two proportional and derivative (PD) feedback controllers.

The two fingertips are sensorized in force. The force sensor is integrated with the base structure of the fingertip. It consists of two circles sharing the same center, as in fig. 2 and rigidly attached with three bars at 120deg. Four strain–gages, glued on each bars, are able to furnish information about the contact force exerted on the disk and the contact point on the disk.

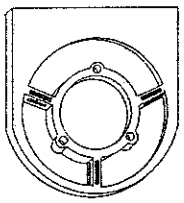

Figure 2: Fingertip built–in force sensor device.

The computational architecture consists of an Intel Pentium machine and a Motorola 68HC11 micro–controller communicating by a standard RS232. The real–time software is distributed on these two machines. More in detail the 68HC11 is charged for the whole sensors and actuators burden, as the A/D and D/A conversions, while the high level control software (cost function optimization, force and position reference generation and others) runs on the main computer. The 68HC11 sampling time of the sensor signals is 4msec.

In the experiment, a tennis table ball is grasped by the two–disk hand as in fig. 3. The contact points (cm) are, in the base frame, $c_1 = [0, 13, 4.5]$ and $c_2 = [3.5, 13, 4.5]$; the contact normal are parallel to the x–axis; the hard–finger model is used for both contacts; the joints axes are parallel to the z axis; $j1 = [0, 0, 0]$ and $j2 = [3.5, 0, 0]$ are the origins of the two joint frames. For the computation of the jacobian and grasp matrix, $\mathbf{J} \in \mathbb{R}^{8\times 2}$ and $\mathbf{G} \in \mathbb{R}^{6\times 8}$, the reader is referred to [9]. As regard the cost function, the limit constraints are set to:

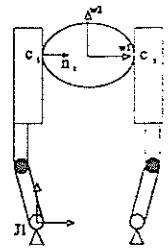

Figure 3: The hand grasping a tennis table.

$f_{i,max}$	$= 10N$
$f_{i,min}$	$= 1N$
μ_i	$= 0.8$

for each contact. The weights $\omega_{i,j}$ of the cost function (14) are equal to one. For the chosen margin $k = 10^{-2}$, the optimization algorithm converges to a minimum value which satisfies the sufficient condition of Proposition 2. The bulk of internal force optimization is carried over each 50msec.

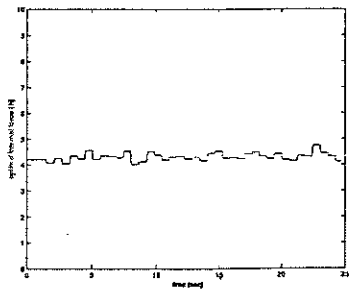

Figure 4: Internal force optimization when no disturbance acts on the object.

In fig. 4 the optimum internal force $\mathbf{A}\widehat{\mathbf{y}}_0$ has been computed in real time for 25sec. In this experiment no disturbance is exerted on the object, $\mathbf{w}_1 = \mathbf{w}_2 = 0$ (fig. 3). Note that the gravity force of the tennis table ball is disregardable and the internal force optimum value is around 4.5N, about the middle of the min–max contact force range.

In the 2nd experiment, an external disturbance $\mathbf{w}_1$ is exerted on the object as in fig. 3 from 15sec to 19sec. As the effect of the external wrench $\mathbf{w}_1$ is sensed by the force

sensors, the output of the optimization algorithm changes in a way that maximizes the distance from contact constraints (minimize the cost function) so guaranteeing the stability of the grasp. The optimum internal force is reported in fig. 5. During the action of $\mathbf{w_1}$, the optimum values increase to about 10N and this corresponds to the instinctive action of squeezing the object to balance $\mathbf{w_1}$.

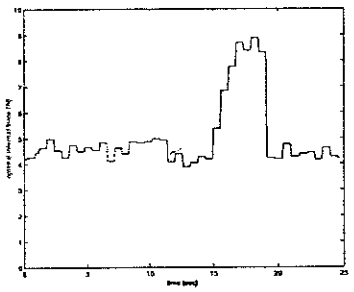

Figure 5: Internal force optimization when the external wrench $\mathbf{w_1}$ acts on the object.

In the last experiment, the external disturbance $\mathbf{w_2}$ (fig. 3) acts from 3sec to 9sec. The optimum internal force is reported in fig. 6. During the action of $\mathbf{w_2}$, the optimum value decreases to about 2.5N and this corresponds to release the grasp in order to do not violate the maximum contact force constraint.

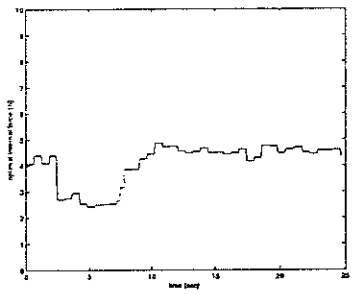

Figure 6: Internal force optimization when the external wrench $\mathbf{w_2}$ acts on the object.

Note that plots in fig. 4, 5 and 6 give the optimum reference for the real internal force which must be send to an internal force controller[9].

8 Conclusion

The optimal synthesis of internal forces in grasps was investigated. The degrees of freedom in choosing the contact forces (6) was exploited to minimize a strictly convex penalty function which weights the risk of violating the contact constraints. A particular attention was devoted to the reachability of internal forces. In fact a basic requirement is that the mechanism is able to control the internal force to the optimum values. In this paper the nonlinear rigid–body dynamics of hand–object device was taken into account. We showed that, in this case, all the forces belonging to the nullspace of the grasp matrix turn to be reachable by hand joints control inputs. Experiments on the two–disk robotic hand were presented.

References

1. A. Bicchi. On the closure properties of robotic grasping. *Int. J. Rob. Res.*, 1995.
2. G. Antognetti. Sviluppo ed implementazione del sistema di controllo per un dspositivo di presa robotico. *Master Thesis, University of Pisa*, 1998.
3. D.E. Orin and S.Y. Oh. Control of force distribution in mechanisms containing closed kinematic chains. *ASME Trans. J. Dyn. Sys. Meas. Contr.*, 102:134–141, June 1981.
4. Y. Nakamura, K. Nagai, and T. Yoshikawa. Dynamics and stability of multiple robot mechanisms. *Int. J. Rob. Res.*, 8(2):44–61, April 1989.
5. D. Prattichizzo, J.K. Salisbury, and A. Bicchi. *Experimental Robotics IV*, "Contact and Grasp Robustness Measures: Analysis and Experiments," pages 83–90. Lecture Notes Contr. Inf. Sci. 223. Springer–Verlag London, 1997.
6. M. Buss, H. Hashimoto, and J. B. Moore. Dextrous hand grasping force optimization. *IEEE Trans. Rob. Aut.*, 12(3):406–418, June 1996.
7. D. Prattichizzo and A. Bicchi. Dynamic analysis of mobility and graspability of general manipulation systems. *IEEE Trans. Rob. Aut.*, 14(2), April 1998.
8. J.K. Salisbury and B. Roth. Kinematic and force analysis of articulated mechanical hands. *J. Mech. Transm. Automat. in Des.*, 105, 1983.
9. D. Prattichizzo and A. Bicchi. Consistent task specification for manipulation systems with general kinematics. *ASME Trans. J. Dyn. Sys. Meas. Contr.*, pages 760–767, December 1997.
10. R.M. Murray, Z. Li, and S.S. Sastry. *A mathematical introduction to robotic manipulation.* CRC, Boca Raton, Florida, 1994.
11. A. Bicchi. Force distribution in multiple whole–limb manipulation. In *Proc. IEEE Int. Conf. Rob. Aut.*, 1993.